Integration
geoscience
engineering
partnership
geoConvention 2013

Interesting directions being pursued in seismic curvature attribute analysis

Satinder Chopra*, Arcis Seismic Solutions, Calgary, Canada
schopra@arcis.com
and
Kurt J. Marfurt, The University of Oklahoma, Norman, OK, USA

Summary

Seismic curvature attribute analysis forms an integral part of most interpretation projects as they yield useful information that adds value for the interpreters. Being a popular tool, curvature applications are expanding in terms of not only different types of curvature measure but also in terms of their visualization, their application on other types of data besides seismic amplitudes, and scaling curvature with other attributes so as to extract more useful information. In this work we discuss the different developments and their applications.

Introduction

Seismic curvature attributes are derived from lateral second-order derivatives of the structural component of seismic time or depth of reflection events. Such a “structural curvature” computation information that may be difficult to see using first-order derivative attributes such as dip magnitude and dip-azimuth. Curvature has long been used by geologists, using both topographic maps and surfaces generated from well tops. Since these attributes were introduced to seismic horizons by Roberts (2001), various types of curvature attributes have been developed and have found their way into commercial software packages.

Interesting directions

Here we describe the interesting directions that are being pursued in terms of not only the optimum applications of these attributes to seismic data, but also the newer developments of these attributes that show promise.

1. *Conditioning of input data.* We begin with the realization that since curvature attributes are second-order derivatives of structural time or depth they tend to enhance not only subtle changes in signal but exacerbate the subtle omnipresent noise in the data. Consequently, to do a good job for curvature attribute computation, the input seismic data needs to be noise-attenuated or conditioned (Chopra and Marfurt, 2008). Random noise inherent in poststack migrated data volumes is perhaps most safely attenuated using edge-preserving structure-oriented filtering. Marfurt (2006) described a multiwindow (Kuwahara) principal component (pc) filter that uses a small volume of data samples to compute the waveform that best represents the seismic data in the spatial analysis window. The output data looks cleaner overall and the vertical faults look sharper. Nonlinear mean, median, alpha-trim mean, and

LUM edge-preserving structure-oriented filters can be more effective when dealing with high energy noise bursts contaminating the data.

When the input data are contaminated by acquisition footprint, whether resulting from acquisition design or introduced by suboptimum processing, it needs to be addressed before attributes are computed on the data. Accentuation of footprint can often be prevented during processing by appropriate interpolation. However, if interpolation becomes computationally prohibitive, other methods are available (Gulunay, 1999; Soubaras, 2001). Chopra and Larsen (2000) suggested the application of narrow k_x-k_y filters on seismic time slices. While this method performs reasonably well, it has a downside in that if the fault/fracture lineament orientations fall in the direction of the footprint, they could get filtered out.

If the seismic data have some type of coherent noise masking the reflection data, dip filtering is used to suppress it, before attribute computation. Figure 1 shows the effect of using dip filters and how the resulting attributes look so much better. Such processes are all referred to as conditioning of the input data.

2. Visualization of seismic attributes. Seismic attributes need to be visualized in such a way that they add value to the seismic interpretation. Many times planar display of seismic attributes are not enough to gauge the precious information we are trying to squeeze out. 3D visualization capability when adopted for seismic data interpretation can be a powerful tool that could integrate the different types of data. *Directional illumination* (or shaded illumination) of interpreted horizons is a powerful means of enhancing subtle fault edges that fall near the limits of seismic resolution (Rijks and Jauffred,1991). The angle at which a given display is illuminated serves to help visualize the data clearly and leads to a detailed level of understanding of the data being interpreted. One of the common *false-color image* techniques used for merging spectral components of seismic data plots three discrete frequencies against red, green and blue (RGB) colors. Features imaged at a higher frequency may be displayed in blue, those imaged at intermediate frequencies displayed in green and the lower frequency component in red. Such a display helps combine more information into one display where we are using the power of the colors for the purpose. The HLS model is more appropriate for color modulation, where one attribute, such as the strike of most-positive curvature, is plotted against hue, and is modulated by a second attribute, such as the value of most-positive curvature, plotted against lightness. *Volume rendering* allows the interpreter to see and interact with features inside 3D volumes in their true 3D perspective. It consists of controlling the color and opacity of each voxel and projecting them onto the image plane. In this manner we bring in shading so as to highlight specific zones, stratal volumes or otherwise sculpted volumes of the 3D seismic data, thereby facilitating the understanding of the spatial disposition of the features of interest. Further manipulation can be effectively used to combine two or more different attribute volumes so that specific features stand out.

3. Computation of curvature attributes on frequency-enhanced data. A common problem with surface seismic data is their relatively low bandwidth which may not serve to achieve the objectives set for the interpretation exercise. Significant efforts are made during processing to enhance the frequency content of the data as much as possible to provide a spectral response that is consistent with the acquisition parameters. Curvature attributes are now being computed on frequency-enhanced seismic data (Chopra and Marfurt, 2010) so that the interpreters have a better understanding of the geology, the play concept and are able to make more meaningful conclusions when it comes to prospect generation.

4. Computation of curvature attributes on impedance data. Poststack and prestack impedance inversion run on seismic volumes remove the effect of the seismic wavelet, modestly increase vertical resolution, compensate for tuning and upward-fining and upward coarsening, and generate volumes that are more tightly correlated to lithology, porosity, and mechanical behavior. Generating coherence from seismic amplitude provides a measure of lateral waveform similarity. The same computation

applied to impedance provides a measure of lateral lithologic similarity (Chopra, 2001). Because the inversion volume has a higher vertical resolution than the input seismic data and enhanced S/N ratio, the coherence resolution from acoustic impedance data is significantly superior to the coherence process applied to seismic data. In a similar way, curvature attributes generated from impedance volumes yield more detail that is useful in interpretation. Figure 2 shows one such comparison.

5. Generating amplitude curvature attributes instead of structural curvature. As stated above the conventional computation of curvature is termed as *structural curvature*, as lateral second-order derivatives of structural component of seismic time or depth of reflection events are used to generate them. Application of lateral second-order derivatives on the amplitudes of seismic data along the reflectors yields *amplitude curvature* (Chopra and Marfurt, 2011). Application of amplitude curvature computation to real seismic data shows higher level of lineament detail as compared with structural curvature, and we show such a comparison in Figure 3. More applications of amplitude curvature and its comparison with structural curvature are discussed in Chopra and Marfurt (2012).

6. *Using Euler curvature.* Euler curvature is a generalization of the dip and strike components of curvature in any user-defined direction. This attribute is useful for the interpretation of lineament features in desired azimuthal directions, say, perpendicular to the minimum horizontal stress (Chopra and Marfurt, 2011). If a given azimuth is known or hypothesized to be correlated with open fractures or if a given azimuth can be correlated to enhanced production or effective horizontal drilling, an Euler-curvature intensity volume can be generated for that azimuth thereby high-grading potential sweet spots. Euler curvature run in desired azimuthal directions can exhibit a more well-defined set of lineaments that may be of interest.

7. *Fracture prediction from scaled curvature attributes.* If we examine curvature on vertical sections, we notice that it has a vertical striping corresponding to the shapes of the seismic reflections. Curvature is a measurement of strain, not of lithology, both of which factors, along with bed thickness, control fractures (Nelson, 2000). Corendering curvature and impedance provides a better fracture indicator (Hunt et al, 2011). Goodway et al. (2006) have shown that the rock's brittleness can be reasonably described by lambda/mu ratio or the closure stress ratio. The elastic rock parameter mu is a measure of the rigidity of the rock and so could be used to scale the curvature in such a way that the scaled attribute still shows the vertical striping and also shows the characteristics of the rigidity estimate. Rocks of different brittleness that have the same curvature value may now be more correctly inferred as having different fracture densities. In Figure 4 we show a section of such a scaled curvature attribute, where the anomaly in the lower middle shows good correlation with the fracture density seen on the log data.

8. Combining seismic azimuthal impedance anisotropy and curvature. It is common knowledge that the existence of fractures and anisotropic stress fields result in velocity variations with azimuth, and hence acoustic impedance. Thus fractures could be estimated by studying reflectivity as a function of azimuth. Impedance data can be generated from seismic data as a function of azimuth (after removing the seismic wavelet and thin-bed tuning effects). In the zone of interest, a horizon is picked on the full stacked volume, and using it as a constraint, horizons are snapped on the azimuth-limited volumes and the minimum and the maximum acoustic impedance values are determined. These then allow the estimation of anisotropy in the zone of interest (Zhang et al., 2010). An overlay of anisotropy over the curvature attribute clearly shows the compartmentalization as we show in Figure 5.

9. Using shape attributes and 3D rose diagrams in seismic interpretation. Once the curvedness of a surface is determined, it is possible to generate different shape attributes such as valley, ridge, dome and bowl attributes. Azimuth of minimum curvature can also be determined from the strike of the valley or the ridge attributes. With these in hand, Chopra et al. (2009) showed that 3D rose diagrams can be

generated for any gridded-square area defined by n-inline by m-crossline analysis window on each horizontal slice. Within each analysis window, we bin each pixel into rose petals according to its azimuth, weighted by its threshold-clipped ridge or valley components of curvedness, then sum and scale them into rose diagrams. The process is repeated for the whole data volume. After that, the rose diagrams are mapped to a rose volume which is equivalent to the data volume and centered in the analysis window, located at the same location as in the input data volume. A robust generation of rose diagrams for the whole lineament volume (corresponding to the seismic volume) is computed, yielding intensity and orientation of lineaments. In Figure 6 we show such 3D rose diagrams at different levels and how they indicate the changes in the orientation of the fractures therein. These rose diagrams can be vector correlated to similar roses from image logs to provide a quantitative prediction of open fracture prediction.

Conclusions

Interpretation workflows of curvature volumes continue to evolve. In addition to structural curvature, curvature can be computed from amplitude, rms amplitude, impedance, lambda-rho, mu-rho, and other inversion volumes. In order to extract meaningful information from seismic attributes, due consideration should be given to pre-conditioning of seismic data and robust dip-steering options. Proper visualization should be done with composite attribute volumes, such as co-rendering volumetric curvature or shape attributes with coherence, provides particularly powerful interpretation tools. Use of shape attributes and 3D rose diagrams aid the interpretation process and facilitate the comparison with image log data. Curvature needs continued calibration with ground truth measurement including microseismic data, production logs, and horizontal image logs.

Curvature attributes are aiding the seismic interpretation process and hopefully we will see many more similar applications in the future.

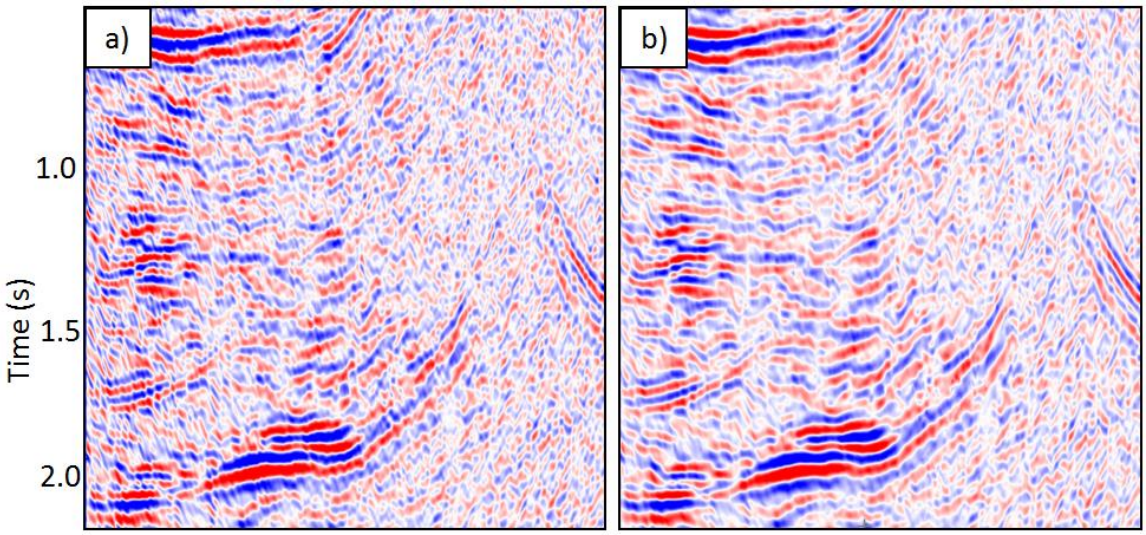

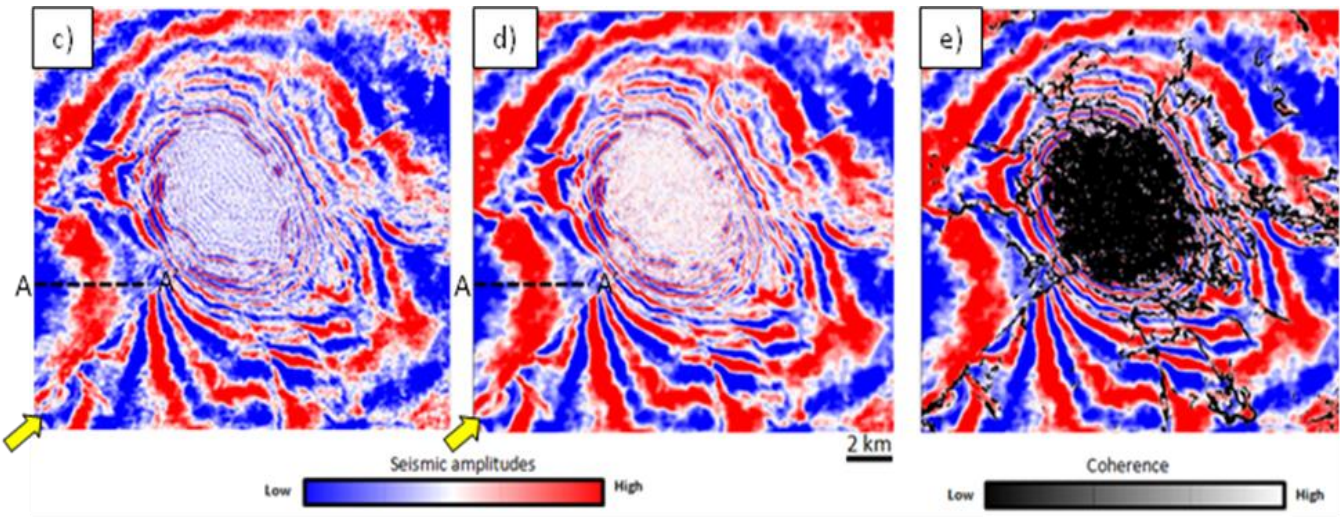

Figure 1*:* Vertical slice AA' through seismic a amplitude volume showing a salt dome (a) before and (b) after structure-oriented filtering and coherent noise suppression. Time slice at t=1.552 s through the same volume (c) before, (d) after structure-oriented filtering, and (e) the seismic time slice morphed with coherence. Note the improved sharpness of one of several radial faults indicated by the yellow arrow. *(Data courtesy of E&B Resources).*

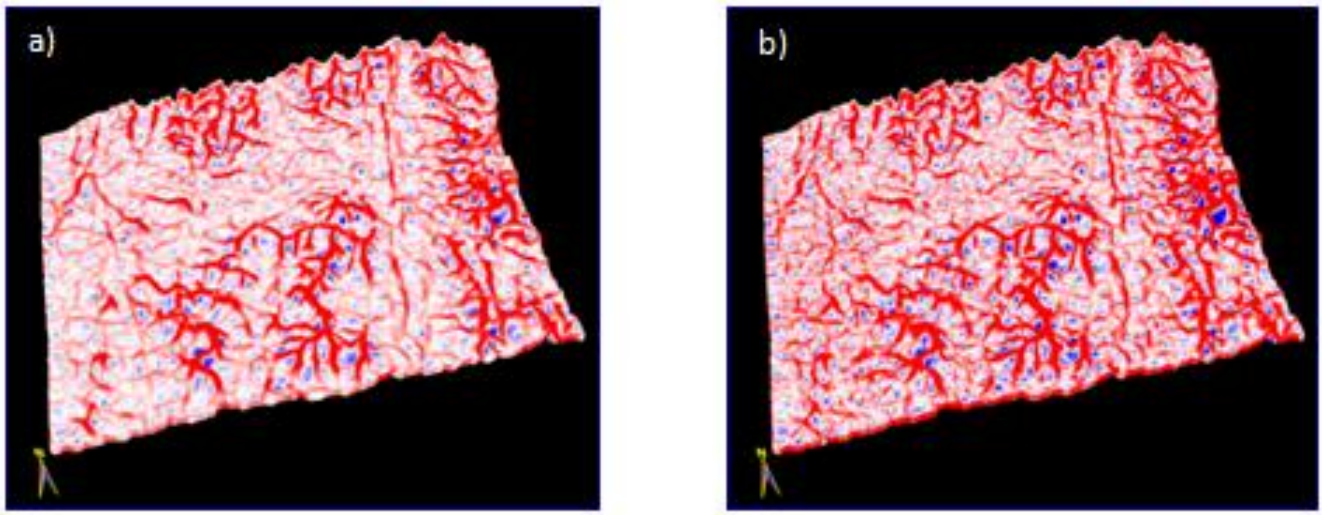

Figure 2*:* Horizon slice through most-positive principal curvature volumes, k_1, computed from (a) the original seismic amplitude data, and (b) from a subsequent model-driven acoustic impedance volume. By using a user-defined source wavelet, model-driven impedance has a flatter spectrum. Constraints applied during inversion act as a filter suppressing random noise.

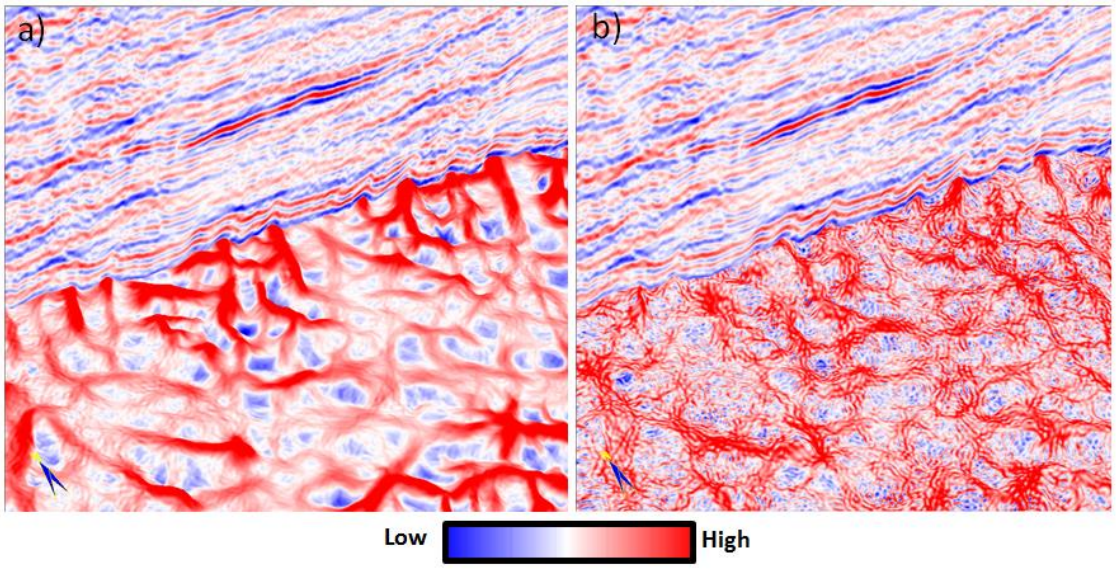

Figure 3: Chair display with seismic section as vertical and a stratal slice 10 ms above the Evie Shale marker from (a) Stratal slice from structural most-positive principal curvature and (b) Equivalent stratal slice from amplitude most-positive curvature.

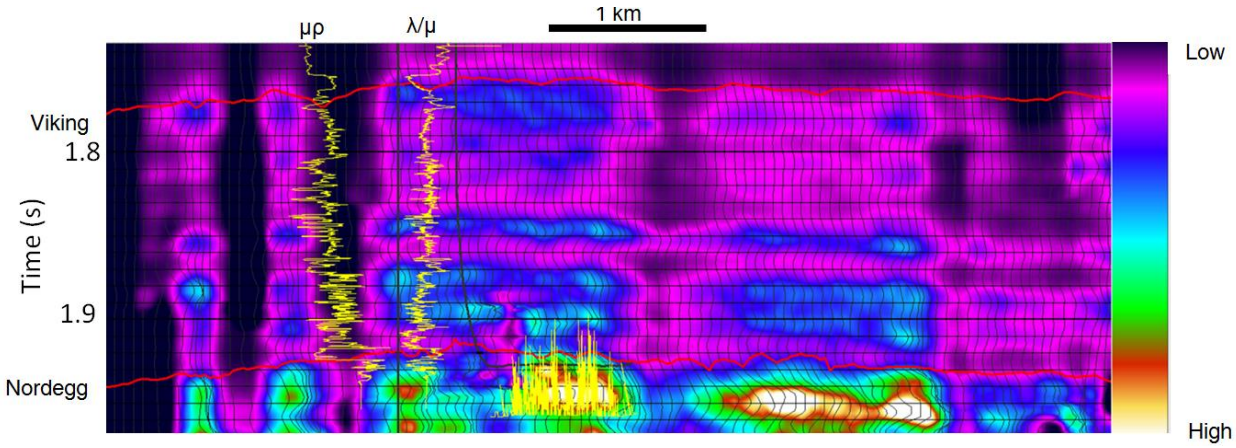

Figure 4: The scaled attribute ($\mu\rho k_1$) combines the vertical-stratigraphic changes in rigidity with the vertical striping of the curvature attribute. This makes more intuitive sense than either attribute alone. *(After Hunt et al., 2011)*

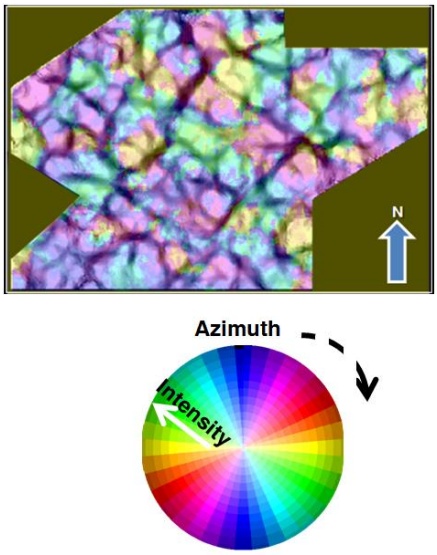

Figure 5: Blended image of k_1 most positive principal curvature and azimuth of maximum stress. Note how the display shows the compartmentalization of the reservoir. *(After Zhang et al., 2011)*

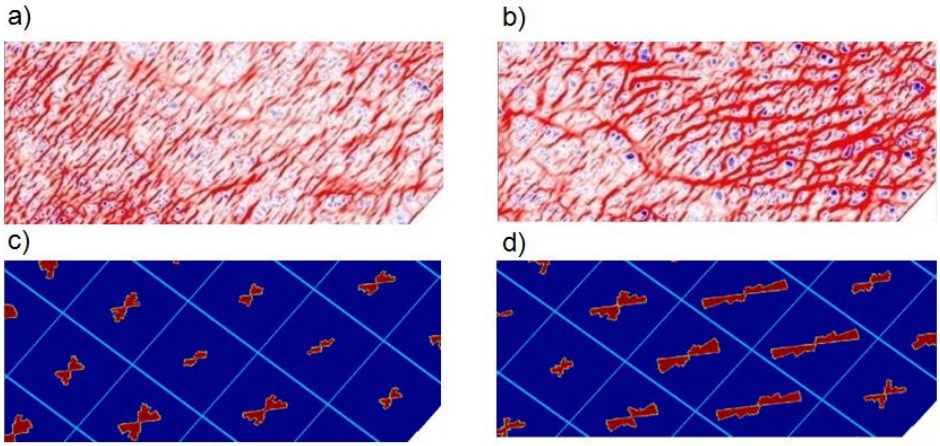

Figure 6: Time slices at (a) t=2.142 and (b) t=2.418 s through k_1 most-positive principal curvature. Time slices through at (a) t=2.142 and (b) t=2.418 s through , the corresponding rose diagram volume. Note the change in the orientation of the lineaments as well as their signature on the roses. *Data courtesy of CGGVeritas Library, Canada.*

Acknowledgements

We thank Arcis Seismic Solutions for encouraging this work and for permission to present these results.

References

1. Anderson, N. L., and E, K, Franseen, 1991, Differential compaction of Winnipegosis reefs: A seismic perspective: Geophysics, **56**, 142-147.
2. Chopra, S. and G. Larsen, 2000, Acquisition footprint — its detection and removal, CSEG Recorder, **25** , no. 8, 16-20.

3. Chopra, S., 2001, Integrating coherence cube imaging and seismic inversion, The Leading Edge, **20**, 354-362.
4. Chopra, S. and K. J. Marfurt, 2008, Gleaning meaningful information from seismic attributes, First Break, 43-53.
5. Chopra, S., K. J. Marfurt and H. T. Mai, 2009, Using automatically generated 3D rose diagrams for correlation of seismic fracture lineaments with similar lineaments from attributes and well log data, First Break, **27**, 37-42.
6. Chopra, S., K. J. Marfurt and S. Misra, 2010, Seismic attributes on frequency-enhanced seismic data, SEG Expanded Abstracts, **29**, 1281-1286.
7. Chopra, S. and K. J. Marfurt, 2011, Structural curvature versus amplitude curvature, SEG Expanded Abstracts, **30**, 980-984.
8. Chopra, S. and K. J. Marfurt, 2012, Seismic attribute expression of differential compaction, SEG Expanded Abstracts.
9. Goodway, W., J., Varsek, and C., Abaco, 2006, Practical applications of P-wave AVO for unconventional gas resource plays-I, CSEG RECORDER, 2006 Special Edition, 90-95.
10. Gulunay, N. ,1999, Acquisition geometry footprints removal. 69th SEG Annual Meeting, Expanded Abstracts, 637-640.
11. Hunt, L., S. Reynolds, T. Brown, S. Hadley, J. Downton and S. Chopra, 2011, Quantitative estimates of fracture density variations: further perspectives, CSEG RECORDER, 36, no. 1, 9-18.
12. Marfurt, K. J., 2006: Robust estimates of reflector dip and azimuth: Geophysics, **71**, P29-P40.
13. Nelson, R. A., 2001, Geologic analysis of naturally fractured reservoirs, Gulf Professional Publishing.
14. Rijks, E. J. H., and J. E. E. M. Jauffred, 1991, Attribute extraction: An important application in any 3-D seismic interpretation: The Leading Edge, **10**, no. 9, 11-19.
15. Roberts, A., 2001, Curvature attributes and their application to 3-D interpreted horizons: First Break, **19,** 85-99.
16. Soubaras, R.,2002, Attenuation of acquisition footprint for nonorthogonal 3D geometries. 72nd SEG Annual Meeting, Expanded Abstracts, 2142-2145.
17. Zhang, K., B. Zhang, J. T. Kwiatkowski and K. J. Marfurt, 2010, Seismic azimuthal impedance anisotropy in the Barnett shale, SEG Expanded Abstracts, 29, 273-277.